iJRASET
International Journal For Research in Applied Science and Engineering Technology



INTERNATIONAL JOURNAL FOR RESEARCH

IN APPLIED SCIENCE & ENGINEERING TECHNOLOGY

Volume: 13 **Issue:** XI **Month of publication:** November 2025

DOI: https://doi.org/10.22214/ijraset.2025.75420

www.ijraset.com

Call: 08813907089 | E-mail ID: ijraset@gmail.com

International Journal for Research in Applied Science & Engineering Technology (IJRASET)
ISSN: 2321-9653; IC Value: 45.98; SJ Impact Factor: 7.538
Volume 13 Issue XI Nov 2025- Available at www.ijraset.com

Feature Based Cancer Detection from QIN Breast DCE-MRI Images

Manushri Deva[1], Sai Prudhvi Karri[2]
Modulus Junior College, Hyderabad, 500085, Telangana, India.

Abstract: ***A single tumor can spread to other locations in the body in an incredibly short time frame of time, often much faster than a number of separate cases can emerge from the single tissue growths. While most doctors believe that MRI is the most widely used imaging technique for detecting breast cancer, there are other alternatives, such as ultrasound and mammography. those patients with previous tests of an evaluations as well as their treatment details were followed up to see whether the previous scans and treatment gave adequate predictions and results were later checked online (QIN, pre-breast images). Extracting feature values from images using the MATLAB function is carried out in a MATLAB macro. Based on the data gathered from the experiment, it, it will be a fairly simple procedure to pinpoint the most important and less important locations Once it is done then it is easy to use MRI segmentation with the Image tool in MATLAB. When developing the methodology, you would need to have in mind the following parameters: Mean Area, Entropy, Mean Absolute Error, Mean Square Error, Peak Signal to Noise Ratio, Standard deviation and Similarity Index were taken into account. It has been shown that the use of function parameters yielded the most efficient results with a minimum of effort and precision.***

Keywords: Image Processing, Magnetic resonance imaging, fuzzy logic, QIN breast DCE

I. INTRODUCTION

A new epidemiological review concludes that breast cancer is the most prevalent form of cancer detected NAT has been advocated in the treatment of locally aggressive stages to assess the down-staging in order to improve the chance of post-resection surgery [1]. Usage of the pathologic full response (pCR) after a standard course of treatment has been associated with long-to-duration benefits such as sickness and survival [2]. Breast cancer is one of the most common cancers in women. a screening MRI for breast cancer usually has a sensitivity of 75-85% However, in the case of denser tissue, it would not have any effect whatsoever (sensitivity 40 percent). Ultrasound used for the early detection of breast cancer is common practice, changes that cannot be observed by magnetic resonance imaging are seen with this technique. There is a high level of diagnostic accuracy when using this tool, as it has a 94-99% sensitivity [3]. When finished, the specificity of MRI of the breast is roughly is around 37 to 86% Because of the high prices, the MRI is only done in some situations. Also, an improved variant of the MRI known as DCE-MRI (Dynamic Contrast Enhancement-Intravenous Contrast MRI) can be used to improve breast screening for women [4]. Most of the tumor lesions show the contrast, in this treatment. To know whether a patient is having an aggressive or unresectable disease, semi-quantically or quantitative pharmacokinetic analysis of DCE-MRI data shows to be more effective than measuring tumor modifications and most commonly utilized [5]. Since it utilizes non-ionizing radiations and intense magnetic fields, as opposed to standard radiations and imaging methods that don't use these two properties.

The use of nuclear magnetic resonance spectroscopy in studying the heart, vaginal, abdominal, and brain soft tissues makes for a clearer picture of the brain, with sharp contrast that enables us to better distinction of tissue MR is segmented using Modified Particle Swarm Optimization, and Area Increasing Algorithm for distinct tumor detection [6]. This is a consistent method of image processing where pixels are calculated by their various characteristics. Texture features are generated by the number of pixels, which categories the texture of the image. Texture analysis methods are used in image processing disciplines such as grouping, segmentation, and extraction of distinct features such as natural tissue, inflammatory areas, and tumors. The research was used to distinguish breast tumors from other breast tissues. However, since different tumors have different patterns, accurate diagnosis remains a challenge. Furthermore, distinguishing between normal and cancerous tissues is difficult at an early stage. As a result, any initiative that aids the clinician in making a correct diagnosis is appreciated and will aid in the saving of peoples. The aim was to verify the method's accuracy by putting it to the test for breast cancer detection using feature extraction with minor feature parameter changes.

©IJRASET: All Rights are Reserved

ISSN: 2321-9653; IC Value: 45.98; SJ Impact Factor: 7.538
Volume 13 Issue XI Nov 2025- Available at www.ijraset.com

II. METHODS

The public dataset "QIN DCE-MRI breast Phased-Array" was derived from The Cancer Archive (TCIA) and is comprised of ten women who were examined using a Siemens 3T IMAT Triple Helix phased-array device, which includes a breast coil and an additional breast coil [7]. DCE-MRI images with echo planar resolution and theta-traced, stochastic axial trajectories (a three-dimensional acquisition with ultrasound) were acquired. Anything in the public record is available for download https://wiki.cancerimagingarchive.net/display/Public/QIN+Breast+DCE-MRI. "QIN-Breast" from The Cancer Imaging Archive is made up of two individuals who had a DCE-MRI conducted using a Siemens 16-SPIM machine and a dedicated breast coil. The obtained recommendation from the oncologist for this kind of NAT based on characteristics of the patients such as menopausal status and tumor scale, as well as nodal status, in advance, as stated. These two breast DCE-MRI studies include a variety of photographs that aid in determining NACC response assessment. Before and after surgery, images were used in a two-stage process. In order to enhance the delineation of the tumor margins, an experienced radiologist (experienced 25 years) was consulted who conducts segmentation on the post-contrast images (dimensions of interest).

Fuzzy logic used to be conceived of as something to be studied by mathematicians and philosophers, but is still used in architecture and technical pursuits today [8]. Fuzzy logic has been used in many areas, such as facial recognition, power conditioners, vacuum cleaners, braking systems, weather forecasts, medical plans, and multi-objective health drug pricing, for instance [9]. Control device architecture, image processing, consumer electronics, and optimization, and robots have made good use of fuzzy logic [10]. It has revived dormant disciplines and raised them to the level of new projects. Multi-valued logic is a logic in which there are more than two values of the property “true” If the proposition has one true extension, it's true; if it has two false extensions, it's false. Fuzzy logic is amorphous is straightforward to grasp, as long as the evidence is approximate [11]. For accomplishing this, fuzzy logic's job of converting input space to output space, a list of rules is evaluated in parallel. These rules are beneficial because they make use of descriptive vocabulary and qualitative concepts as well as well as objective ones. Fuzzy controller (FL) comprises a fuzz unit, Defuzzification, and post-processing subsystems [12].

A. Fuzzy Logic In Digital Image Processing

Fuzzy image processing is based on image analysis, image representation, segmentation, and image processing, as fuzzy sets. Selecting and using the right Fuzzy technique decide what is shown and what has to be achieved results in the best image representation and processing. Fig. 2 shows the three primary techniques for Fuzzy image processing: (Fuzzy the image), modifying the membership values, and if possible, De-fuzzy the image [13].

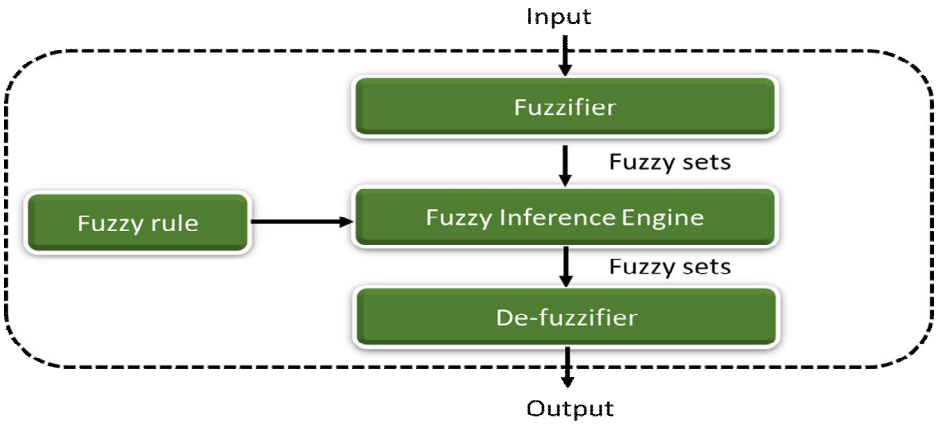


Fig.2 Fuzzy Logic System (FLS)

The fuzzification and defuzzification measures are important because there is no hardware that's even close to being fuzzy. fuzzy approaches to filter photographs Fuzzy photos analysis yield the key advantages in the middle step (modification of membership values). Using fuzzy methods, the affiliation values are after the image data has been converted to the grey level plane (de-fuzzing). Fuzzy clustering may be rule-based, rule-based, or fuzzy logic-based [14]. In this study, a novel FIS system, that doesn't require the calculation of a threshold values, is proposed for edge detection in digital images is used. It starts with a 3x3 binary matrix partitioning of the images. When applied directly, a fuzzy inference method discovered the set of values for the edges of the matrix floating about in the space [15].

©IJRASET: All Rights are Reserved | SJ Impact Factor 7.538 | ISRA Journal Impact Factor 7.894 |

B. Feature Extraction

This work pays special attention to both geometrical and texture characteristics. This segment explains the main features. Geometric characteristics are the most accessible, but most significant in the study of breast cancer. Most generally, MR images are used to classify these elements.

1) *Mean Area:* The sum of all of a number range reflects the average of the quantities (Pixels). A ROI includes pixel values and the intensity of the image's colour. The algorithm can be mathematically modelled as a 2D matrix of pixels. Mean value decides the light of the area of ROI [16].
2) *Entropy:* The degree of chaos or randomness of a system attains is proportional to the entropy of the system includes. Visual texture is almost like entropy. The total entropy of the image must be zero if the texture is smooth. With the level of randomness, the sharpness of the picture decreases [17].
3) *Standard Deviation:* The variance is defined as the divergence of a data set from its mean. The data collection has a large variation means that it is further from the mean, and the less the variation, the closer to the mean it is. A major deviation in the normal growth rate of breast tumors does not exist [18]. MATLAB's 'std2' built-in feature returns a standard deviation Eq. (1).

$$\text{Standard Deviation} = \sqrt{\frac{\sum_{i=1}^{n}(x_i - \bar{x})^2}{n-1}} \quad (1)$$

Where, x_i=Value of the ith point in the data set, $\bar{x}$=The mean value of the data set, n=The number of data points in the data set

4) *Pixel-Signal Noise ratio:* The noise tolerance of a picture has if the signal-to-to-noise ratio is high, the resulting picture is effectively noise-free. If you send the subject a picture of the size (or height, or width) of the highest possible number of pixels, MAXI is equivalent to the pixel values of the given MR image (Usually 255) [19]. It is essential that the perceptual similarity rating (PSNR) is between 40 to 60 dB. Represented in Eq. (2).

$$PSNR = 10log_{10}\frac{MAX_I^2}{MSE} \quad (2)$$

5) *Mean Absolute Error (MAE):* MAE is the sum of the overall percentage error values between the actual and segmented images [20] and is denoted in Eq. (3).

$$\text{MAE value} = \frac{1}{n}\sum_{i=1}^{n}|y_i - \bar{y}| \quad (3)$$

Where, x_i= Predicted value of the ith point in the data set, $\bar{x}$=The actual value of the data set, n=The number of data points in the data set

6) *Mean Square Error (MSE):* Measuring the initial and derivative values is referred to as MSE. In statistics, the number of the squares of the errors is used as an expression to refer to an error total The MSE is the sum of the squared errors in the segmented image minus the sum of the squares of the displacements [21] and is denoted in Eq. (4).

$$\text{MSE value} = \frac{1}{mn}\sum_{i=0}^{m-1}\sum_{j=0}^{n-1}[I(i,j) - K(i,j)]^2 \quad (4)$$

Results segmentation values of the non-segmented images should be reduced. the lower MSE values characterize the probability of an image segmentation problem. The m and n in the images describe the number of rows and columns of each image. To put it another way, "I" and "K" are the input and the output images. More segmentation yields improved results.

7) *Dice (SI-Similarity Index):* Dice is expressed as a percentage and varies from 100 to 0% to 0% to 1000%. This sense the regions in the input image and explains the parallels between them [22]. The values used to calculate SI are denoted in Eq. (5):

$$SI = \frac{2\,X\,CI}{2\,X\,CI\,X\,F\,X\,FN} \quad (5)$$

Where, Tumor area observed (CI) and allocated A false (F) tumor was found in the input image area of the patient's image. An imaging analysis was performed on the patient's tumor image to search for the tumor but could not find it or it was misclassified as something else (FN).

It is on clinical and surgical experience of a radiologist that CI, F, and FN are extracted from recognizing a tumor's location. A MATLAB generated a feature vector which provides enough classifications of the image, using all of the aforesaid parameters. knowledge and pattern parameters that effectively characterize the picture.

III.RESULT AND DISCUSSION

A. Designing Fuzzy Inference System

The formula used to compute the membership values is depicted as below, after we have identified the most appropriate set of rules, we are setting up the fuzzy system to meet our needs. Fuzzy architecture involves the two essential stages: Fuzzy description and fuzzy rule development. A MF denotes how each input point is related to a particular membership value (or degree) on the scale [23]. Therefore, the MFP was constructed with an MF in mind. The authors have made the decision to transform the input data to a fuzzified value on the right here below. Each of the vertices of a triangle MF can be considered as a part of a fuzzy set containing A (a: lower boundary and c: upper boundary where membership degree is zero, b: the center where membership degree is 1). An essential part of fuzzy sets is to be able to decide on the MFs and determine their degree of membership. MF can occur in several different forms, although some standard implementations can serve as examples. Distance vectors are transferred to FLS as (dxij and dyij) after the segmentation. The initial vector was transformed to discrete input ranges called discretization [24]. Distance value is discretized is a method of translating value from 0 to 1 unit range. This paper divides each pixel's maximum value (Max_p) into 0 to 1 measure.

The formula for calculating the values is as follows:

$$\widehat{y_{ij}} - \frac{y_{ij}}{Max_p} \quad (6)$$

The results from Equation (6) allow one to individually change all of the pixel values within a given range. Now, the latest values from 0 to 1 can be found. So, all values that fall in the range are then replaced with the scaled values. As a consequence, the discretized picture I gets blurred

$$\widehat{y_{ij}} = \begin{cases} A & 0 < y_{ij} < 1 \\ P & 0 < y_{ij} < 0.5 \\ D & 0 < y_{ij} < 1 \end{cases} \quad (7)$$

Yij is the target pixel in the ith test image, A is the mean db value of the measured image, and P is the PSNR value If the discrete function finds that an element in the input file only includes A and D, the element ID (I, j) is discretized.

Sample rules

If (Area is Negative) and (PSNR is Negative) and (DICE is Negative) then (Decision is Negative)
If (Area is Positive) and (PSNR is Negative) and (DICE is Negative) then (Decision is Positive(I))
If (Area is Positive) and (PSNR is Positive) and (DICE is Negative) then (Decision is Positive (II))
If (Area is Positive) and (PSNR is Positive) and (DICE is Positive) then (Decision is Positive (II))

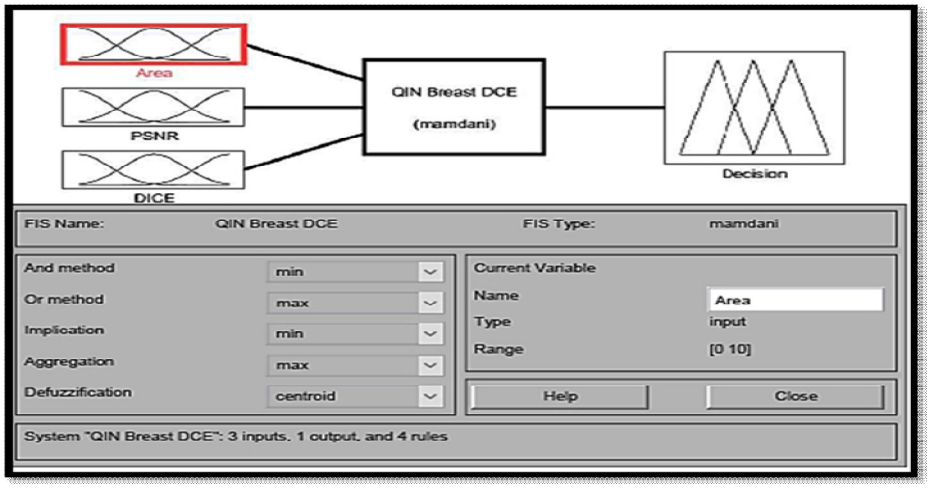


Fig.3 Fuzzy Inference System (FIS) rules

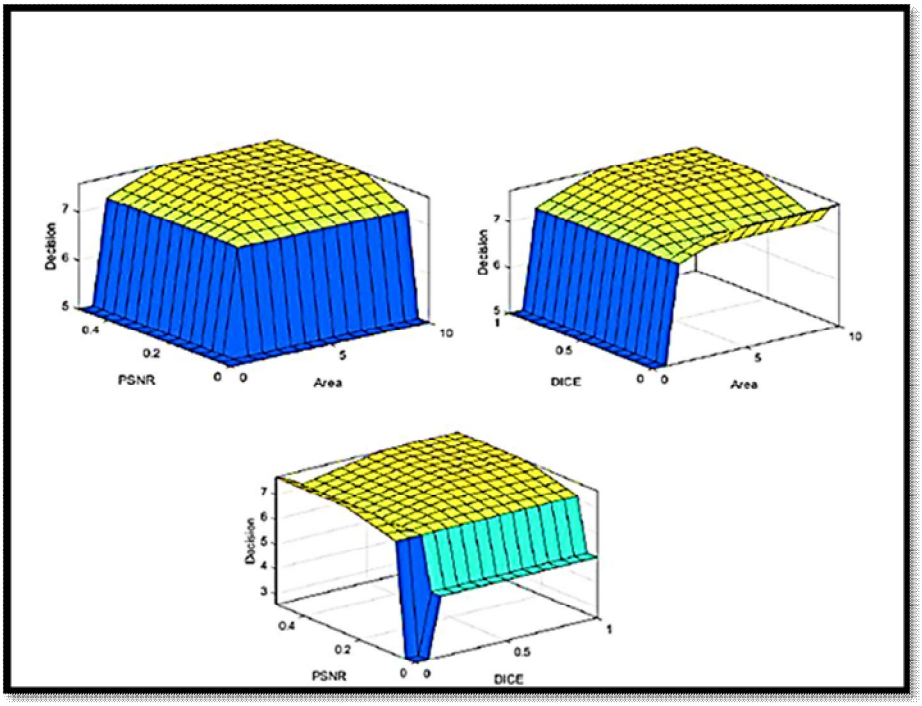


Fig.4 Sample of Output images of QIN Breast DCE MRI from surface viewer in 'jpg'

Table 1 shows the feature parameters of QIN Breast DCE-MRI images (1-5) after segmentation of ROI. When analyzing Table 1, Mean Area of images 1 to 5 were calculated as 55883, 58030, 5.6232e+04, 5.6582e+04 and 5.6419e+04, Entropy were identified as 2.4835, 1.7334, 0.9930, 2.4823 and 2.5008, Mean Absolute Error (MAE) were found to be 5.4121, 11.9073, 12.1160, 3.9495 and 4.5044, Mean Square Error (MSE) were calculated as 382.6684, 1.3360e+03, 1.2910e+03, 266.1686 and 292.5680, Peak Signal to Noise Ratio (PSNR) identified as 0.1258, 0.0360, 0.0373, 0.1808 and 0.1645, Standard deviation (SD) evaluated as 2.1410e+04, 2.7359e+04, 1.6410e+04, 1.7924e+04 and 2.3172e+04 and Similarity Index 00.4344, 0.4104, 0.4299, 0.4281 and 0.4289.

Table 1: Feature parameters derived from sample set from QIN Breast DCE-MRI images

Sample	Mean area	Entropy	Standard Deviation	Pixel-Signal Noise ratio (db)	Mean Absolute Error (MAE)	Mean Square Error (MSE)	Dice
Image 1	55883	2.4835	2.1410e+04	0.1258	5.4121	382.6684	0.4344
Image 2	58030	1.7334	2.7359e+04	0.0360	11.9073	1.3360e+03	0.4104
Image 3	5.6232e+04	0.9930	1.6410e+04	0.0373	12.1160	1.2910e+03	0.4299
Image 4	5.6582e+04	2.4823	1.7924e+04	0.1808	3.9495	266.1686	0.4281
Image 5	5.6419e+04	2.5008	2.3172e+04	0.1645	4.5044	292.5680	0.4289

The suggested technique derives features from a function-extracted QIN MRI feature contrast. Additionally, the PSNR result is seen for five separate images, and compared to that of the original and ROI segmented image in Table 1. When applying process, the best PSNR of 0.1808 db for the smallest number of pixels in the table. Furthermore, output of MSE is found to be less on image 4 as calculated by the resemblance index (Dice), the image quality improves. MSE has estimated that the error on test picture 4 is the lowest to put it another way, the noise level goes up, along with the size of the picture. Via our trial, we've understood our proposed system obviously outperforms all other methods in PSNR and MSE.

©IJRASET: All Rights are Reserved | SJ Impact Factor 7.538 | ISRA Journal Impact Factor 7.894 |

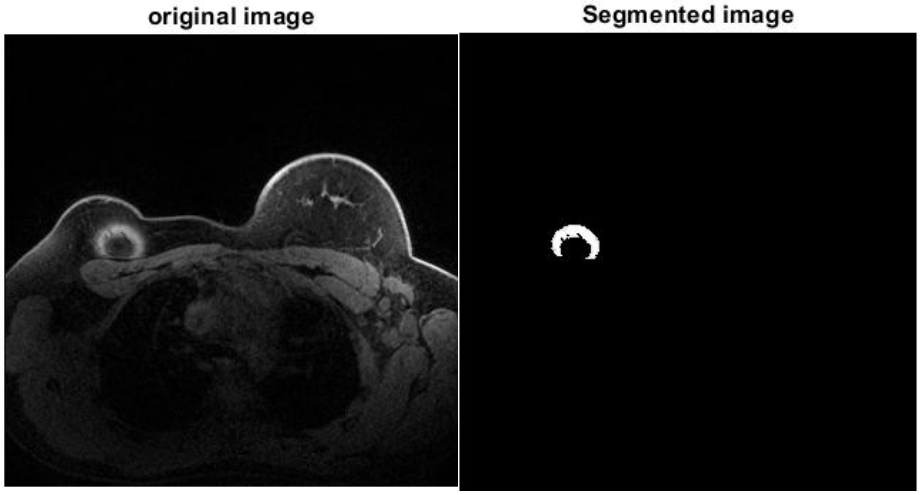


Fig.2 Sample of Input & Output images of QIN Breast DCE MR in 'jpg'

IV. CONCLUSIONS

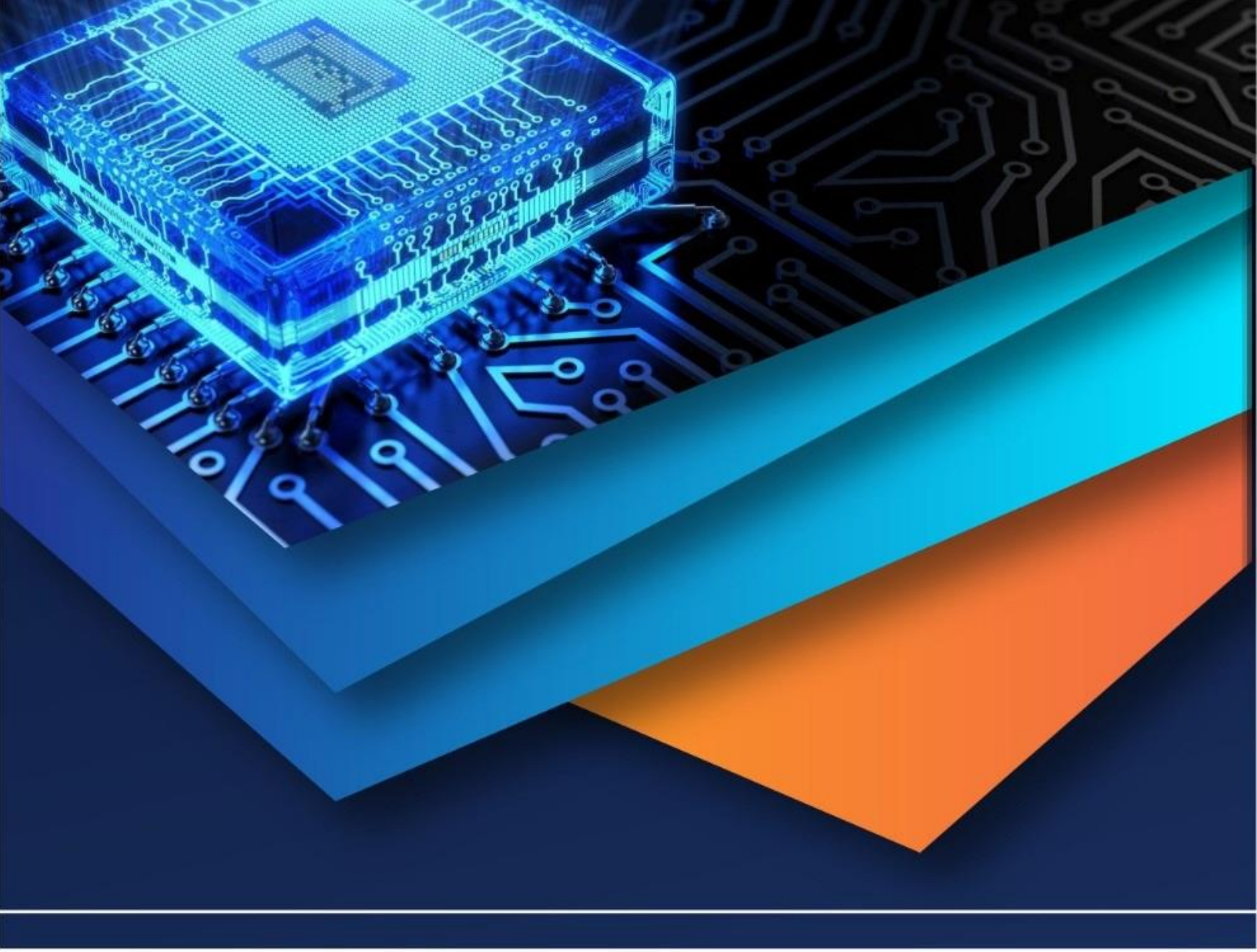
In this study, a Fuzzy Logic–based image processing system was successfully designed and implemented for the detection and analysis of breast cancer using QIN Breast DCE-MRI datasets. The proposed method effectively integrates Fuzzy Inference Systems (FIS) with feature extraction techniques to enhance tumor segmentation and diagnostic accuracy. The fuzzy-based segmentation technique overcomes the limitations of traditional threshold-based methods by handling image uncertainty and noise more efficiently. From the obtained results, key image quality parameters such as Mean Area, Entropy, Standard Deviation, PSNR, MAE, MSE, and Dice Similarity Index were computed to evaluate the performance of the system. Among the tested samples, Image 4 demonstrated the best performance, exhibiting the highest PSNR (0.1808 dB) and the lowest MSE (266.1686), indicating superior segmentation quality and reduced error levels. The results confirm that the proposed approach produces clearer, more reliable tumor delineation with improved similarity to the ground truth. Overall, the study demonstrates that integrating fuzzy logic with DCE-MRI feature analysis provides an efficient and intelligent framework for breast cancer detection. This technique enhances image segmentation accuracy, reduces computational errors, and offers robust performance even under varying noise conditions. Future work may extend this approach by incorporating machine learning classifiers or deep learning frameworks for automated diagnosis and larger dataset validation to further improve diagnostic reliability and clinical applicability.

REFERENCES

[1] K. U. Park et al., "Neoadjuvant endocrine therapy use in early stage breast cancer during the covid-19 pandemic," Breast Cancer Res. Treat., pp. 1–10, 2021.
[2] X. Sun et al., "Neoadjuvant therapy and sentinel lymph node biopsy in HER2-positive breast cancer patients: results from the PEONY trial," Breast Cancer Res. Treat., pp. 1–6, 2020.
[3] T. Huzarski et al., "Screening with magnetic resonance imaging, mammography and ultrasound in women at average and intermediate risk of breast cancer," Hered. Cancer Clin. Pract., vol. 15, no. 1, pp. 1–8, 2017.
[4] D. M. Bardo, D. R. Biyyam, M. C. Patel, K. Wong, D. Van Tassel, and R. K. Robison, "Magnetic resonance imaging of the pediatric mediastinum," Pediatr. Radiol., vol. 48, no. 9, pp. 1209–1222, 2018.
[5] T. P. Siegel, G. Hamm, J. Bunch, J. Cappell, J. S. Fletcher, and K. Schwamborn, "Mass spectrometry imaging and integration with other imaging modalities for greater molecular understanding of biological tissues," Mol. Imaging Biol., vol. 20, no. 6, pp. 888–901, 2018.
[6] D. A. Ragab, M. Sharkas, S. Marshall, and J. Ren, "Breast cancer detection using deep convolutional neural networks and support vector machines," PeerJ, vol. 7, p. e6201, 2019.
[7] S. Punitha, A. Amuthan, and K. S. Joseph, "Benign and malignant breast cancer segmentation using optimized region growing technique," Future Comput. Inform. J., vol. 3, no. 2, pp. 348–358, 2018.
[8] V. Vaishnavi and M. Suresh, "Applications of Fuzzy Logic Approach for Assessment," in Advances in Materials Research, Springer, 2021, pp. 1191–1198.
[9] A. Mardani et al., "Application of decision making and fuzzy sets theory to evaluate the healthcare and medical problems: a review of three decades of research with recent developments," Expert Syst. Appl., vol. 137, pp. 202–231, 2019.
[10] J. Greeda, A. Mageswari, and R. Nithya, "A study on fuzzy logic and its applications in medicine," Int. J. Pure Appl. Math., vol. 119, no. 16, pp. 1515–1525, 2018.
[11] P. Hilletofth, M. Sequeira, and A. Adlemo, "Three novel fuzzy logic concepts applied to reshoring decision-making," Expert Syst. Appl., vol. 126, pp. 133–143, 2019.
[12] D. N. Utama and U. Taryana, "Fuzzy logic for simply prioritizing information in academic information system," Int. J. Mech. Eng. Technol., vol. 10, no. 2, pp. 1594–1602, 2019.

[13] C. Challoumis, "Multiple Axiomatics Method and the Fuzzy Logic," Available SSRN 3224425, 2018.
[14] G. Kaiser, "Mathematical modelling and applications in education," Encycl. Math. Educ., pp. 553–561, 2020.
[15] F. Gunawan, G. Wang, D. N. Utama, and S. Komsiyah, "Decision Support Model for Supplier Selection Using Fuzzy Logic Concept," in 2018 International Conference on Information Management and Technology (ICIMTech), IEEE, 2018, pp. 394–399.
[16] D. Sathish, S. Kamath, K. Prasad, R. Kadavigere, and R. J. Martis, "Asymmetry analysis of breast thermograms using automated segmentation and texture features," Signal Image Video Process., vol. 11, no. 4, pp. 745–752, 2017.
[17] S. Saman and S. J. Narayanan, "Survey on brain tumor segmentation and feature extraction of MR images," Int. J. Multimed. Inf. Retr., vol. 8, no. 2, pp. 79–99, 2019.
[18] H. M. Whitney, H. Li, Y. Ji, P. Liu, and M. L. Giger, "Comparison of Breast MRI Tumor Classification Using Human-Engineered Radiomics, Transfer Learning From Deep Convolutional Neural Networks, and Fusion Methods," Proc. IEEE, vol. 108, no. 1, pp. 163–177, 2019.
[19] Q. Liu, Z. Liu, S. Yong, K. Jia, and N. Razmjooy, "Computer-aided breast cancer diagnosis based on image segmentation and interval analysis," Automatika, vol. 61, no. 3, pp. 496–506, 2020.
[20] A. Ibrahim, S. Mohammed, H. A. Ali, and S. E. Hussein, "Breast cancer segmentation from thermal images based on chaotic Salp swarm algorithm," IEEE Access, vol. 8, pp. 122121–122134, 2020.
[21] B. Z. Dashevsky et al., "Breast implant-associated anaplastic large cell lymphoma: Clinical and imaging findings at a large US cancer center," Breast J., vol. 25, no. 1, pp. 69–74, 2019.
[22] F. Sadoughi, Z. Kazemy, F. Hamedan, L. Owji, M. Rahmanikatigari, and T. T. Azadboni, "Artificial intelligence methods for the diagnosis of breast cancer by image processing: a review," Breast Cancer Targets Ther., vol. 10, p. 219, 2018.
[23] M. Fayaz, I. Ullah, and D. Kim, "An optimized fuzzy logic control model based on a strategy for the learning of membership functions in an indoor environment," Electronics, vol. 8, no. 2, p. 132, 2019.
[24] Z. Ashraf, M. L. Roy, P. K. Muhuri, and Q. D. Lohani, "Interval type-2 fuzzy logic system-based similarity evaluation for image steganography," Heliyon, vol. 6, no. 5, p. e03771, 2020.

©IJRASET: All Rights are Reserved | SJ Impact Factor 7.538 | ISRA Journal Impact Factor 7.894 |



10.22214/IJRASET

45.98

IMPACT FACTOR: 7.129

IMPACT FACTOR: 7.429

INTERNATIONAL JOURNAL FOR RESEARCH

IN APPLIED SCIENCE & ENGINEERING TECHNOLOGY

Call : 08813907089 (24*7 Support on Whatsapp)